

# SuperSpec: On-Chip Spectrometer Design, Characterization, and Performance

J. Redford<sup>1</sup> •• P. S. Barry<sup>2</sup> • C. M. Bradford<sup>3</sup> • S. Chapman<sup>4</sup> • J. Glenn<sup>5</sup> •
S. Hailey-Dunsheath<sup>3</sup> • R. M. J. Janssen<sup>3</sup> • K. S. Karkare<sup>6</sup> • H. G. LeDuc<sup>3</sup> •
P. Mauskopf<sup>7</sup> • R. McGeehan<sup>6</sup> • E. Shirokoff<sup>6</sup> • J. Wheeler<sup>8</sup> • J. Zmuidzinas<sup>1</sup>

Received: 2 November 2021 / Accepted: 30 August 2022 / Published online: 26 September 2022 © The Author(s), under exclusive licence to Springer Science+Business Media, LLC, part of Springer Nature 2022

#### **Abstract**

SuperSpec is an integrated, on-chip spectrometer for millimeter and sub-millimeter astronomy intended to pave the way for large-scale, multi-beam spectrometer instruments. SuperSpec is demonstrating a three beam, dual-polarization instrument for observing star formation in distant galaxies on the Large Millimeter Telescope, a 50 m telescope on Volcan Sierra Negra in Mexico. SuperSpec provides moderate resolution ( $R \sim 270 - 290$ ) in the 1 mm atmospheric window (200–300 GHz) with a lithographically patterned filterbank on a 3.5 cm x 5.5 cm chip. The filterbank intended for deployment is implemented in niobium, fed by a lensed antenna, and using a extremely low-volume  $(2.6\mu m^3)$  titanium nitride lumped element kinetic inductor detectors (LEKIDs) as the sensors. The small size of the spectrometer and inherent multiplexibility of the kinetic inductance detectors will allow the future use of SuperSpec in larger, multi-pixel/multi-object spectrometers far beyond the threepixel spectrometer being demonstrated soon. We report the design of the spectrometer, laboratory characterization of devices for the upcoming SuperSpec deployment. This involves laboratory testing of the filterbank spectral response, and observing noise in the TiN KIDs.

- California Institute of Technology, Pasadena, CA 91125, USA
- Argonne National Laboratory, Lemont, IL 60439, USA
- Jet Propulsion Laboratory, Pasadena, CA 91109, USA
- <sup>4</sup> University of British Columbia, Vancouver, BC, Canada V6T 1Z4
- Goddard Space Flight Center, Greenbelt, MD 20771, USA
- <sup>6</sup> University of Chicago, Chicago, IL 60637, USA
- Arizona State University, Tempe, AZ 85281, USA
- National Institute of Standards and Technology, Boulder, CO 80303, USA



**Keywords** KIDs · Millimeter-wave · Spectrometer · Filterbank

### 1 Introduction

SuperSpec is a compact, on-chip millimeter-wave spectrometer. The millimeter and sub-millimeter wavelengths are important for probing star formation and galactic dynamics in the early universe, because UV and optical radiation produced by stars get absorbed and reprocessed by dust into far-IR. The gas-phase interstellar medium cools through several emission lines, including the [CII] 158µm fine-structure transition, a broad indicator of star formation [1-3]; CO rotational transitions that cool molecular gas; and [NII] 205  $\mu m$  fine-structure transition, which traces ionized gas. These and others spectral lines are redshifted into the trans-millimeter bands for much of cosmic history; in particular [CII] lies in the 200-300 GHz band for redshift 5-9, the late stages of reionization. While ALMA is very sensitive for observing these lines one-by-one in individual galaxies, the survey speed of a wide-band, moderate-resolution spectrometer with many spatial beams can vastly exceed that of ALMA. There are several groups creating an on-chip spectrometer, along with SuperSpec, such as DESHIMA, which has already demonstrated an on-chip filterbank on sky, though in a different frequency range [4] and  $\mu$  – Spec [5] is using a dispersion-based spectrometer on-chip, able to be compact due to the high index of refraction of silicon. Such a capability can be used for both pointed multi-object spectroscopy of galaxies [6], as well as for line intensity mapping (LIM), for which pioneering instruments such as TIME [7] and SPT-SLIM (Karkare et al. these proceedings) are now being built. Lithographically patterned on-chip spectrometers will enable the ultimate potential of these measurements: filled 2-D focal plane arrays in which each pixel is a background-limited spectrometer. We present progress on our implementation of this technology, SuperSpec, with a particular emphasis on the titanium-nitride (TiN) KIDs used in the device.

# 2 Device Design and Performance

SuperSpec is an on-chip microstrip filterbank with half-wave resonators illustrated schematically with the circuit diagram in Fig. 1. The length of the microstrip resonator is stepped logarithmically along the filterbank to fill the full bandwidth. Each channel's bandwidth is determined by the total quality factor, including the couplings between the resonator to the half-wave filter and the filter to the TiN KID inductor, along with the dielectric loss. The optimization of these parameters is handled numerically and detailed in Redford et al. [8].

The devices described in this paper are 110-channel spectrometer chips covering the 200 to 300 GHz band, the chip design is detailed in Fig. 2, and some of the channels' spectral profiles are shown in Fig. 1. The fact that there is a difference in heights of the spectral profiles, with one half having less response than the other half, is due to a mask error causing the filterbank to have the resonators out of order. This causes half the filterbank to get more power at the expense of the



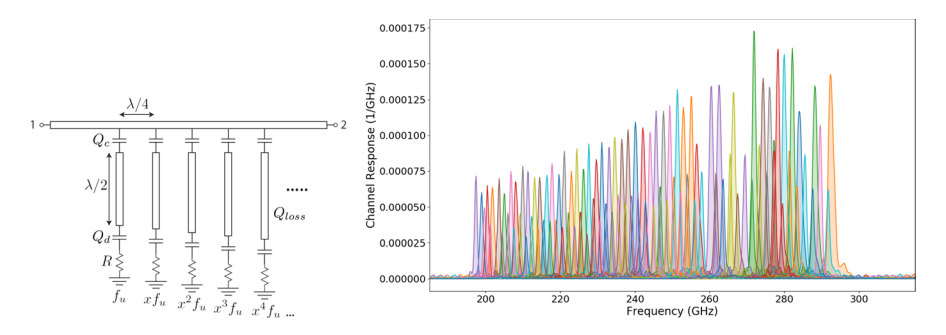
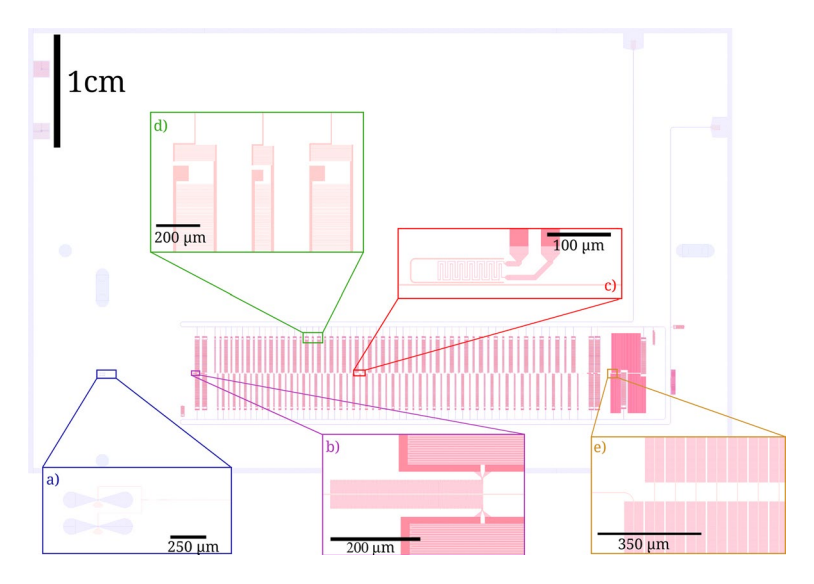


Fig. 1 Left: A circuit diagram of the SuperSpec filterbank. A series of half-wave resonators are coupled to a microstrip feedline, with the length of the half-wave resonators stepped to cover the full band. The total resonator Q, set by the coupling  $Q(Q_c)$  to the feedline, the loss to the dielectric  $(Q_{loss})$ , and the coupling to the detector  $(Q_d)$ , set the single channel bandwidth. The detector is shown as a resistor in the circuit diagram since it is a dissipative element. Right: The spectral profiles of channels in a 110-channel prototype chip. Due to a mask error causing the half-wave resonators to be out of order, one half of the resonators get a larger share of the power at the expense of the other half. Additionally, the variation of the gap energy of the TiN across the die and the dielectric loss causes the variation in peak heights with frequency



**Fig. 2** A breakdown of the 110 channel SuperSpec chip. The filterbank covers 200 – 300 GHz and the total die is 3.5 by 5 cm. Panel **a** shows the dual-slot antenna that couples radiation onto the microstrip feedline. For diagnostic purposes, panel **b** shows a KID coupled to the microstrip without a half-wave resonator, giving it a broadband optical response. Panel **c** shows a section of the filterbank, the half-wave resonators that provide spectral selectivity are wrapped around the inductor of the KIDs. Panel **d** shows the end of the interdigitated capacitors of the KIDs and the coupling capacitors of the KIDs which consists of an interdigitated capacitor to the readout microstrip line and a parallel plate capacitor to the ground plane. Panel **e** shows a TiN meanders that absorb remaining power that is not absorbed by the filterbank



other half, though the strong overlap between adjacent channels means that this only has a minimal effect on the overall sensitivity. This mask error has been corrected, and new devices are to be produced and studied. The additional variation in peak height across the band is due to the parabolic gap energy variation in the TiN film [9, 10] and the dielectric loss in the microstrip. With capacitor clipping [11], we were able to remove frequency collisions due to gap variations across the die. We have previously demonstrated background limited detectors with Super-Spec [10–12], but have been challenged in obtaining good optical efficiency.

The optical efficiency of our current devices and instrument has room for improvement. But at audio frequencies above several Hertz, the NEP is dominated by photon noise. This is comparable to the SuperSpec chop frequency of our modulating mirror, for which the speed and duty cycle must be traded. Therefore, the detector low frequency (1/f) noise has the potential to negatively impact the performance on-sky and will be the subject of the following section.

## 3 Inductor 1/f Noise

It has been previously remarked that there is some excess 1/f noise in TiN KIDs including our reactive sputtered non-stoichiometric films [9, 13, 14]. Examples of this are shown in Fig. 3 showing the noise PSDs of a spectral channel looking at two different optical loadings, a 293K room temperature load and a mirror reflecting the beam back into the interior of the cryostat. The effective temperature of the was found to be  $61 \pm 1$ K. Additionally, the stage temperature was varied from the normal operating base temperature of 217mK. We find a dependence on optical loading, but interestingly, find little or no dependence on device temperature, indicating that the mechanism does not depend in a straightforward way on quasiparticle density.

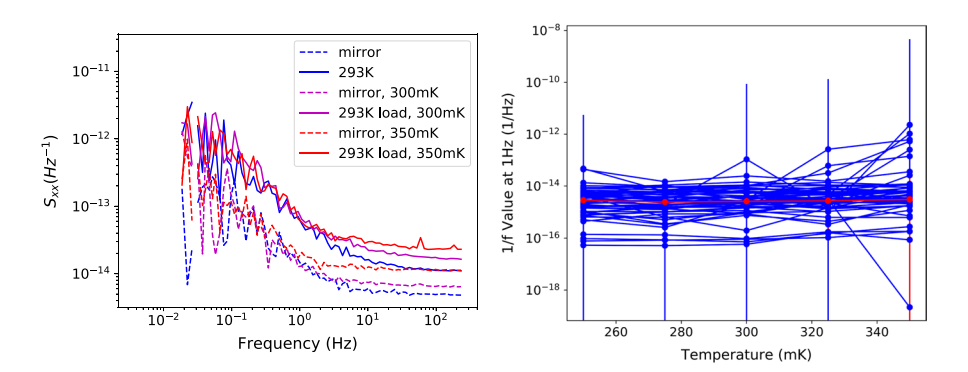


Fig. 3 Left, the  $S_{xx}$  plots of a representative resonator with two blackbody loadings and three-stage temperatures. To obtain the lowest blackbody temperatures, a mirror was used to reflect the beam back into the interior of the cryostat, and the loading of the mirror is found to be  $61 \pm 1K$ . Right, the fitted temperature and loading scalings of the 1/f noise in filterbank resonators of a deployment candidate. The median value for each temperature is in red



# 4 Photon Noise and Sensitivity

And the fitted GR levels of  $S_{xx}$  along with the difference in noise with changes in loading show that SuperSpec is limited by photon noise. The expression for photon noise of a blackbody is

$$NEP_{\text{phot}} = hv \sqrt{\delta v \eta_{\text{opt}} n(\eta_{\text{opt}} n + 1)}$$
 (1)

where  $\nu$  is the center frequency,  $\delta\nu$  is the bandwidth of the channel,  $\eta_{\rm opt}$  is the optical efficiency between the source and the detector, and n is the photon occupation number. In the case of SuperSpec, the lensed antenna system couples to a single optical mode. So, the photon occupation of the source, for a beam filling load, is a Bose–Einstein distribution. The equation presented is the typical expression for the noise at the detector. To refer this to the noise at the input of the instrument, one has to divide the previous NEP by the optical efficiency. This is the more meaningful figure of merit for the instrument's performance on-sky. This gives the equation

$$NEP_{\text{phot,front}} = h\nu\sqrt{\delta\nu n(n+\frac{1}{\eta})}$$
 (2)

For a KID, the change in noise from a change in optical loading also includes excess recombination noise from generated quasiparticles. But the excess recombination noise can be expressed as an enhancement of the shot noise [15]. Starting with the responsivity  $\mathcal{R}$  and recombination noise found in Zmuidzinas [16].

$$NEP_{\rm rac}^2 = S_{\rm xx, rec} * \mathcal{R}^{-2} \tag{3}$$

$$=\frac{2V\Delta^2\delta n_{qp}}{\tau_{qp}\eta_{opt}^2\eta_{ph}^2}(1+\frac{\tau_{qp}}{\tau_{\max}})\tag{4}$$

$$\delta n_{qp} = \frac{\eta_{pb} \tau_{qp} \eta_{\text{opt}}}{\Lambda V} P_{inc}$$
 (5)

$$=\frac{\eta_{pb}\tau_{qp}}{\Delta V}h\nu\delta\nu\eta n_{\rm phot} \tag{6}$$

$$NEP_{rec}^{2} = \frac{2\Delta}{\eta_{pb}h\nu} NEP_{shot}^{2} (1 + \frac{\tau_{qp}}{\tau_{max}})$$
 (7)

$$\delta NEP^2 = h^2 v^2 \delta v (\delta(n^2) + \frac{3\delta n}{\eta})$$
 (8)

where the last equation comes from assuming the minimum pair breaking efficiency, meaning only one pair of quasiparticles are generated from a photon  $(\eta_{pb} = \frac{2\Delta}{hv})$ .



And, make the assumption that the quasiparticle lifetime is set by  $\tau_{max}$ , making the increase in square recombination noise equal to double the increase of the shot noise. This  $\tau_{max}$  limited lifetime has been previously observed in SuperSpec TiN KIDs [9–11, 15] and demonstrated in the bottom left panel of Fig. 4. Using this equation, the difference in the noise under two loadings can give an upper bound of the optical efficiency (since the pair breaking efficiency was assumed to be the minimum).

## 5 Conclusion

SuperSpec is currently in preparation for the instrument deployment at the Large Millimeter Telescope. The instrument is ready with several 110 channel chips that cover 200–300 GHz band to demonstrate a 3-pixel spectrometer on-sky. Devices are currently photon noise limited, with individual spectral channels having an NEP of

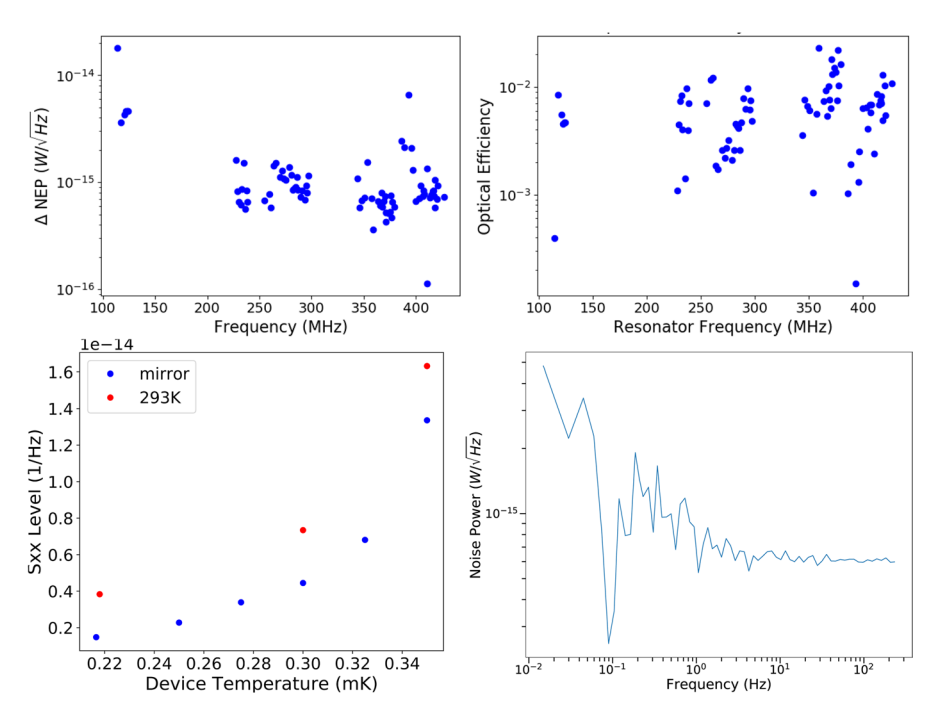


Fig. 4 Top left, the difference in NEP measured for the change in loading from the 293K, room temperature load, to the  $\sim 61$  K mirror load, causing the instrument to look at the cold interior of the cryostat. Top right, the upper bound of the optical efficiency calculated from the photon noise difference to the right. For both plots the channels below 150 MHz are the broadband channels, with the lower efficiency being positioned after the filterbank, coupling to power not absorbed by the filterbank. Bottom left, the  $S_{xx}$  of a spectral channel at various temperatures and two optical loadings, the difference between the loadings shows that the optical responsivity is constant, as predicted by previous measurements demonstrating that the quasiparticle lifetime is constant. Bottom right, the NEP PSD of a representative spectral channel, the NEP at the chopping frequency during telescope observations is  $\sim 8 * 10^{-16} W / \sqrt{Hz}$ 



less than  $10^{-15}W/\sqrt{Hz}$ , at a loading similar to expected on-sky loadings. And further enhancements to the sensitivity of the instrument will have to be obtained from increasing optical throughput.

Acknowledgments This work is supported in part by NASA Grant 399131.02.06.05.11

#### References

- D. Schaerer, M. Ginolfi, M. Béthermin, Y. Fudamoto, P.A. Oesch, O. Le Fèvre, A. Faisst, P. Capak, P. Cassata, J.D. Silverman, Lin Yan, G.C. Jones, R. Amorin, S. Bardelli, M. Boquien, A. Cimatti, M. Dessauges-Zavadsky, M. Giavalisco, N.P. Hathi, S. Fujimoto, E. Ibar, A. Koekemoer, G. Lagache, B.C. Lemaux, F. Loiacono, R. Maiolino, D. Narayanan, L. Morselli, Hugo Méndez-Hernàndez, F. Pozzi, D. Riechers, M. Talia, S. Toft, L. Vallini, D. Vergani, G. Zamorani, E. Zucca, The ALPINE-ALMA [CII] survey: no or weak evolution in the [CII]-SFR relation over the last 13 Gyr. Astron. Astrophys. 643, A3 (2020). https://doi.org/10.1051/0004-6361/202037617
- A. Boselli, G. Gavazzi, J. Lequeux, D. Pierini, [CII] at 158μm as a star formation tracer in the latetype galaxies. Astron. Astrophys. 385, 454–463 (2002). https://doi.org/10.1051/0004-6361:20020 156
- G. Stacey, N. Geis, R. Genzel, J.B. Lugten, A. Poglitsch, A. Sternberg, C.H. Townes, The 158-Micron [Cii] line: a measure of global star formation activity in galaxies. Astrophs. J. 373, 423 (1991)
- T. Takekoshi, K. Karatsu, J. Suzuki, Y. Tamura, T. Oshima, A. Taniguchi, S. Asayama, T.J.L.C. Bakx, J.J.A. Baselmans, S. Bosma, J. Bueno, K.W. Chin, Y. Fujii, K. Fujita, R. Huiting, S. Ikarashi, T. Ishida, S. Ishii, R. Kawabe, T.M. Klapwijk, K. Kohno, A. Kouchi, N. Llombart, J. Maekawa, V. Murugesan, S. Nakatsubo, M. Naruse, K. Ohtawara, A. Pascual Laguna, K. Suzuki, D.J. Thoen, T. Tsukagoshi, T. Ueda, P.J. de Visser, P.P. van der Werf, S.J.C. Yates, Y. Yoshimura, O. Yurduseven, A. Endo, DESHIMA on ASTE: on-sky responsivity calibration of the integrated superconducting spectrometer. J. Low Temp. Phys. 199(1–2), 231–239 (2018). https://doi.org/10.1007/s10909-020-02338-0
- P.A.R. Ade, C.J. Anderson, E.M. Barrentine, N.G. Bellis, A.D. Bolatto, P.C. Breysse, B.T. Bulcha, G. Cataldo, J.A. Connors, J.P.W. Cursey, N. Ehsan, H.C. Grant, T.M. Essinger-Hileman, L.A. Hess, M.O. Kimball, A.J. Kogut, A.D. Lamb, L.N. Lowe, P.D. Mauskopf, J. McMahon, M. Mirzaei, S.H. Moseley, J.W. Mugge-Durum, O. Noroozian, U. Pen, A.R. Pullen, S. Rodriguez, P.J. Shirron, R.S. Somerville, T.R. Stevenson, E.R. Switzer, C. Tucker, E. Visbal, C.G. Volpert, E.J. Wollack, S. Yang, The experiment for cryogenic large-aperture intensity mapping (EXCLAIM). J. Low Temp. Phys. 199(3–4), 1027–1037 (2020). https://doi.org/10.1007/s10909-019-02320-5
- C.M. Bradford, S. Hailey-Dunsheath, E. Shirokoff, M. Hollister, C.M. McKenney, H.G. LeDuc, T. Reck, S.C. CHapman, A. Tikhomirov, T. Nikola, J. Zmuidzinas. X-Spec: A Multi-Object trans-millimeter-wave spectrometer for CCAT. *Proc. SPIE* 91531Y (2014)
- A.T. Crites, J.J. Bock, C.M. Bradford, T.C. Chang, A.R. Cooray, L. Duband, Y. Gong, S. Hailey-Dunsheath, J. Hunacek, P.M. Koch, C.T. Li, R.C. O'Brient, T. Prouve, E. Shirokoff, M. Silva, Z. Staniszewski, B. Uzgil, M. Zemcov. The TIME-Pilot intensity mapping experiment *Proc. SPIE* 9153 (2014)
- J. Redford, J. Wheeler, K. Karkare, S. Hailey-Dunsheath, C.M. Bradford, E. Shirokoff, P.S. Barry, G. Che, J. Glenn, H.G. Leduc, P. Mauskopf, R. McGeehan, T. Reck, J. Zmuidzinas, The design and characterization of a 300 channel, optimized full-band millimeter filterbank for science with Super-Spec. Procc. SPIE. 10708, 187–194 (2018)
- J. Wheeler, Millimeter-Wave Galaxy Spectroscopy: SuperSpec On-Chip Spectrometer Technology Development and ALMA Observation of Molecular Gas in the Arp 220 Nucleus, Doctoral dissertation, University of Colorado, Boulder, 2019
- J. Wheeler, S. Hailey-Dunsheath, E. Shirokoff, P.S. Barry, C.M. Bradford, S. Chapman, G. Che,
   J. Glenn, M. Hollister, A. Kovács, H.G. LeDuc, P. Mauskopf, R. McGeehan, C.M. McKenney,
   R. O'Brient, S. Padin, T. Reck, C. Ross, C. Shiu, C.E. Tucker, R. Williamson, J. Zmuidzinas,



- SuperSpec: development towards a full-scale filter bank. Procc. SPIE (2016). https://doi.org/10. 1117/12.2233798
- R. McGeehan, P.S. Barry, E. Shirokoff, C.M. Bradford, G. Che, J. Glenn, S. Gordon, S. Hailey-Dunsheath, M. Hollister, A. Kovács, H.G. LeDuc, P. Mauskopf, C. McKenney, T. Reck, J. Redford, C. Tucker, J. Turner, S. Walker, J. Wheeler, J. Zmuidzinas, Low-temperature noise performance of superspec and other developments on the path to deployment. J. Low T. Phys. 193(5–6), 1024–1032 (2018). https://doi.org/10.1007/s10909-018-2061-6
- J. Wheeler, S. Hailey-Dunsheath, E. Shirokoff, P.S. Barry, C.M. Bradford, S. Chapman, G. Che, S. Doyle, J. Glenn, S. Gordon, M. Hollister, A. Kovács, H.G. LeDuc, P. Mauskopf, R. McGeehan, C. McKenney, T. Reck, J. Redford, C. Ross, C. Shiu, C. Tucker, J. Turner, S. Walker, J. Zmuidzinas, SuperSpec, the on-chip spectrometer: improved NEP and antenna performance. J. Low T. Phys. 193(3–4), 408–414 (2018). https://doi.org/10.1007/s10909-018-1926-z
- 13. J. Gao. Twenty Years of Microwave Kinetic Inductance Detectors: A Technical Review. Presented at the 18th Conference for Low Temperature Detectors, Milan, Italy, (2019)
- M.R. Vissers, J.E. Austermann, M. Malnou, C.M. McKenney, B. Dober, J. Hubmayr, G.C. Hilton, J.N. Ullom, J. Gao, Ultrastable millimeter-wave kinetic inductance detectors. Appl. Phys. Lett. 116, 3, 032601 (2020). https://doi.org/10.1063/1.5138122
- S. Hailey-Dunsheath, E. Shirokoff, P.S. Barry, C.M. Bradford, S. Chapman, G. Che, J. Glenn, M. Hollister, A. Kovács, H.G. LeDuc, P. Mauskopf, C. McKenney, R. O'Brient, S. Padin, T. Reck, C. Shiu, C.E. Tucker, J. Wheeler, R. Williamson, J. Zmuidzinas, Low noise titanium nitride kids for superspec: a millimeter-wave on-chip spectrometer. J. Low Temp. Phys. 184(1–2), 180–187 (2016). https://doi.org/10.1007/s10909-015-1375-x
- J. Zmuidzinas, Superconducting microresonators: physics and applications. Ann. Rev. Condens. Matter Phys. 3(1), 169–214 (2012). https://doi.org/10.1146/annurev-conmatphys-020911-125022

**Publisher's Note** Springer Nature remains neutral with regard to jurisdictional claims in published maps and institutional affiliations.

Springer Nature or its licensor holds exclusive rights to this article under a publishing agreement with the author(s) or other rightsholder(s); author self-archiving of the accepted manuscript version of this article is solely governed by the terms of such publishing agreement and applicable law.

